

Chitosan–Silica Composite Aerogel for the Adsorption of Cupric Ions: Isothermal Remodeling and MOORA-Based Model Selection

Mohd Yunus Shukor^{1*}

¹Department of Biochemistry, Faculty of Biotechnology and Biomolecular Sciences, Universiti Putra Malaysia, 43400 UPM Serdang, Selangor, Malaysia.

*Corresponding author:

Mohd Yunus Shukor,

Department of Biochemistry,

Faculty of Biotechnology and Biomolecular Sciences,

Universiti Putra Malaysia,

43400 UPM Serdang,

Selangor,

Malaysia.

Email: mohdyunus@upm.edu.my

HISTORY

Received: 29th Nov 2024
Received in revised form: 28th Dec 2024
Accepted: 31st Dec 2024

KEYWORDS

Remodel
Chitosan
Isotherm
Brouers-Sotolongo
MOORA

ABSTRACT

A remodeling evaluation was conducted on the sorption isotherm data for copper adsorption onto chitosan–silica composite aerogel (Vareda et al., 2024) using nonlinear regression due to the irregular manner in which the regression was done and reported. The remodelling exercise results showed that the top five were Koble-Corrigan, Brouers–Sotolongo, Fritz-Schlunder III, Hill, and Sips models. The Brouers–Sotolongo model was the most precise in estimating the maximum adsorption capacity (q_m) because it considers the surface's heterogeneity and offers narrow confidence intervals. On the other hand, the Langmuir model chosen in the original publication had wide confidence intervals, which means that it was less precise. In addition, the study also stresses the need to use various error functions to improve the model selection and increase the validity of the models. In addition, for the first time, to the best of our knowledge, this study reported on the first use of Multiobjective Optimization by Ratio Analysis (MOORA) method for isothermal model selection and ranking in the adsorption field. This approach simplifies the selection process by systematically evaluating and ranking the numerous isotherm and kinetic models that are commonly used in adsorption research. Therefore, this study recommends using advanced and flexible isotherm models such as Brouers-Sotolongo for accurate adsorption modeling but also stresses the need for rigorous statistical validation in adsorption research. The results of this study can be used to enhance the accuracy of adsorption studies in wastewater treatment, environmental remediation, and material science applications.

INTRODUCTION

Nonlinear regression of adsorption isotherm data presents significant challenges when working with small datasets (six points or fewer), particularly in assessing residual normality, heteroscedasticity, and randomness. Normality tests such as Shapiro-Wilk and Anderson-Darling typically require larger datasets (≥ 10 points) to provide meaningful results [1]. Their statistical power is often insufficient for small datasets, making it difficult to distinguish between normal and non-normal distributions. Even when normality is assumed, small sample sizes can skew residual distributions, leading to misinterpretation of model performance. Another prevalent issue in adsorption studies is heteroscedasticity, where residual variance is non-constant, particularly when data spans a wide concentration range. Traditional tests such as Bartlett's, Levene's, and White's are unreliable for small datasets, making visual methods like residual versus fitted value plots more commonly used, albeit subjective. If left unaddressed, heteroscedasticity can

significantly distort nonlinear regression analysis, leading to misleading conclusions [2]. To assess residual randomness, the runs test is often employed, detecting systematic patterns in residuals that may indicate model misspecification. However, with datasets containing six or fewer points, the test produces limited runs, reducing statistical confidence. Small sample sizes elevate the risk of Type I and Type II errors, making the test unreliable in distinguishing true randomness [3]. Due to these limitations, traditional validation methods may not be robust enough for small adsorption datasets. To compensate, incorporating multiple error functions into model selection improves reliability despite dataset size constraints. This highlights the necessity for complementary statistical approaches to ensure model accuracy and reliability.

Beyond these statistical challenges, selecting an appropriate adsorption isotherm or kinetic model remains difficult due to the vast number of available models and evaluation criteria. Conventional model selection methods primarily rely on a single

evaluation metric, such as the coefficient of determination (R^2) or the sum of squared errors (SSE). However, these metrics alone fail to provide a holistic view of model performance across multiple dimensions [4,5].

To improve model selection, multiple error functions can be used to assess model accuracy from different perspectives. The adjusted R^2 [6] accounts for model complexity, making it more reliable for comparing models with different parameter counts. However, it still does not penalize overfitting as effectively as information-theoretic criteria like the corrected Akaike Information Criterion (AICc) [7,8] and the Bayesian Information Criterion (BIC) [9]. AICc corrects for small sample sizes, preventing overfitting while maintaining a good data fit, whereas BIC imposes a stricter penalty on model complexity, favoring simpler, more generalizable models. Hannan and Quinn's Criterion (HQ) [10] serves as a compromise between AICc and BIC, applying a logarithmic penalty to balance goodness-of-fit and complexity.

Additional statistical functions further enhance model assessment. Root Mean Squared Error (RMSE) quantifies the average residual deviation, though it is sensitive to large errors. Marquardt's Percent Standard Deviation (MPSD) [11–13] normalizes errors based on model complexity, providing a more balanced metric. Bias Factor (BF) and Accuracy Factor (AF) (Ross, 1996) assess systematic deviation and predictive reliability, respectively. A BF value of 1 indicates an unbiased model, while an AF value close to 1 suggests high predictive accuracy. These error functions, widely reported in adsorption research, ensure that model selection accounts for overfitting risks, predictive power, and overall goodness-of-fit [14–17].

The Multiobjective Optimization by Ratio Analysis (MOORA) method provides a powerful methodology for handling this complexity by utilizing many objectives during decision-making. MOORA is one of the Multi-Criteria Decision-Making (MCDM) and also include other methods such as Analytic Hierarchy Process (AHP) [18], Technique for Order Preference by Similarity to Ideal Solution (TOPSIS) [19], Preference Ranking Organization Method for Enrichment Evaluation (PROMETHEE) [20] and Weighted Sum Model (WSM) [21,22]. Of these, the MOORA method offers advantages in terms of simplicity and efficiency for small datasets as its direct ratio-based approach by aggregating normalized performance values removes subjective preference assignments or complex iterative calculations inherent in the other methods making it easier to apply in small datasets [23,24].

MOORA ranks adsorption models using a decision matrix that integrates multiple performance metrics. Weights are assigned to each criterion, and models are ranked based on normalized performance scores. Unlike conventional model selection, which may prioritize a high R^2 value despite large SSE deviations, MOORA considers multiple, often conflicting, indicators to ensure a well-rounded evaluation [25–29]. While MOORA has been applied in adsorption research for adsorbent selection in CO_2 capture [30], it has not yet been used to rank isotherm or kinetic models. Other MCDM methods, such as AHP and TOPSIS, have been applied in adsorption research, but these applications focused on selecting adsorbents based on cost, safety, accessibility, and reusability, rather than explicitly ranking nonlinear adsorption models based on error functions [31]. Integrating multiple criteria into model selection enhances objectivity, ensuring transparent and reproducible decisions. MOORA's ability to balance multiple statistical measures, including error functions, model complexity penalties, and

performance accuracy, makes it an ideal tool for adsorption studies. To date, MOORA has not been employed for adsorption isotherm or kinetic model ranking, making this study a pioneering effort. We demonstrate MOORA's effectiveness in our remodeling of a previous adsorption study [32], which relied on an inconsistent application of error function analysis for determining the best adsorption model for copper binding to chitosan–silica composite aerogels. By adopting MOORA for model selection, adsorption researchers can ensure more reliable and systematic progress in evaluating adsorption models, reducing subjectivity while maintaining computational efficiency, especially in small datasets. Future research should explore the integration of MCDM frameworks with traditional error functions to create a more comprehensive and objective model selection process in adsorption studies.

METHODS

Data acquisition and fitting

Figure 4b data from a previously published study [32] was digitized using the freeware Webplotdigitizer 2.5 [33]. The program's digitization capabilities have garnered accolades for their reliability [34]. Then, Curve-Expert Professional (Version 2.6.5, copyright Daniel Hyams), a program for curve fitting, was used to perform nonlinear regression on the data. MATLAB software package (Mathworks, Massachusetts, USA) was used to resolve the implicit equations.

Statistical analysis

This study employed the following statistical discriminatory or error functions tests; HQ (Hannan and Quinn's Criterion) [10], Bias Factor (BF), Accuracy Factor (AF) [63], root-mean-squared error (RMSE), adjusted coefficient of determination (R^2) [6], corrected Akaike Information Criterion (AICc) [7,8], Marquardt's percent standard deviation (MPSD) [11–13] and Bayesian Information Criterion (BIC) [9]. In general, n is the total number of observations, Ob_i and Pd_i are the predicted and observed values, and p is the total number of parameters of the model [64].

RMSE was calculated using the following formula;

$$RMSE = \sqrt{\frac{\sum_{i=1}^n (Pd_i - Ob_i)^2}{n-p}} \quad (\text{Eqn. 1})$$

BF and AF were calculated using the following formula;

$$\text{Bias factor} = 10 \left(\sum_{i=1}^n \log \frac{(Pd_i / Ob_i)}{n} \right) \quad (\text{Eqn. 2})$$

$$\text{Accuracy factor} = 10 \left(\sum_{i=1}^n \log \frac{|(Pd_i / Ob_i)|}{n} \right) \quad (\text{Eqn. 3})$$

AICc was calculated using the following formula;

$$AICc = 2p + n \ln \left(\frac{RSS}{n} \right) + \frac{2(p+1)+2(p+2)}{n-p-2} \quad (\text{Eqn. 4})$$

BIC was calculated using the following formula;

$$BIC = n \ln \left(\frac{RSS}{n} \right) + k \ln(n) \quad (\text{Eqn. 5})$$

HQC was calculated using the following formula;

$$HQC = n \ln \left(\frac{RSS}{n} \right) + 2k \ln(\ln n) \quad (\text{Eqn. 6})$$

Adjusted coefficient of determination (R^2) was calculated using the following formula;

$$Adjusted (R^2) = 1 - \frac{RMS}{S^2} \quad (\text{Eqn. 7})$$

$$Adjusted (R^2) = 1 - \frac{(1-R^2)(n-1)}{(n-p-1)} \quad (\text{Eqn. 8})$$

MPSD was calculated using the following formula;

$$MPSD = 100 \sqrt{\frac{1}{n-p} \sum_{i=1}^n \left(\frac{Ob_i - Pd_i}{Ob_i} \right)^2} \quad (\text{Eqn. 9})$$

Isotherms

Due to the low number of data points, only models (**Table 1**) with parameters limited to three were deemed appropriate to prevent overfitting.

Table 1. Mathematical models in the remodelling data [35,36].

| Isotherm | p | Formula | Ref. |
|----------------------|-----|--|--------------------|
| Henry's law | 1 | $q_e = HC_e$ | [37] |
| Langmuir | 2 | $q_e = \frac{q_{mL} b_L C_e}{1 + b_L C_e}$ | [35] |
| Jovanovic | 2 | $q_e = q_{mJ} (1 - e^{-K_J C_e})$ | [38] |
| Freundlich | 2 | $q_e = K_F C_e^{n_F}$ | [39] |
| Dubinin-Radushkevich | 2 | Incorrect form $q_e = q_{mDR} \exp \left\{ -K_{DR} \left[RT \ln \left(1 + \frac{1}{C_e} \right) \right]^2 \right\}$ correct form $q_e = q_{mDR} \exp \left\{ -K_{DR} \left[RT \ln \left(\frac{C_s}{C_e} \right) \right]^2 \right\}$ | [40,41] [42,43] |
| Koble-Corrigan | 3 | $q_e = \frac{AC_e^n}{1 + BC_e^n}$ | [44] |
| Temkin | 3 | $q_e = \frac{RT}{b_T} \{ \ln(a_T C_e) \}$ | [45,46] |
| Redlich-Peterson | 3 | $q_e = \frac{K_{RP1} C_e}{1 + K_{RP2} C_e^{\beta_{RP}}}$ | [47] |
| Sips | 3 | $q_e = \frac{K_S q_{mS} C_e^{n_S}}{1 + K_S C_e^{n_S}}$ | [48] |
| Toth | 3 | $q_e = \frac{q_{mT} C_e}{(K_T + C_e^{n_T})^{1/n_T}}$ | [49] |
| Hill | 3 | $q_e = \frac{q_{mH} C_e^{n_H}}{K_H + C_e^{n_H}}$ | [50] |
| Khan | 3 | $q_e = \frac{q_{mK} b_K C_e}{(1 + b_K C_e)^{a_K}}$ | [51] |
| BET | 3 | $q_e = \frac{q_{mBET} \alpha_{BET} C_e}{(1 - \beta_{BET} C_e)(1 - \beta_{BET} C_e + \alpha_{BET} C_e)}$ | [52] |
| Vieth-Sladek | 3 | $q_e = \frac{q_{mVS} b_{VS} C_e}{(1 + b_{VS} C_e)^{n_{VS}}}$ | [53] |
| Radke-Prausnitz | 3 | $q_e = \frac{A_{RP} B_{RP} C_e^{\beta}}{A_{RP} + B_{RP} C_e^{\beta-1}}$ | [54-56] |
| Brouers-Sotolongo | 3 | $q_e = q_{mBS} \left[1 - \left(1 + (0.5) \left(\frac{t}{\tau} \right)^\alpha \right)^{-2} \right]$ | [57-59] |
| Fritz-Schlunder-III | 3 | $q_e = \frac{q_{mFS} K_{FS} C_e}{1 + K_{FS} C_e^{n_{FS}}}$ | [60] |
| Fowler-Guggenheim* | 3 | $q_e = q_{mFG} \frac{K_L C_e e^{\frac{\alpha q_e}{q_{mFG}}}}{1 + K_L C_e e^{\frac{\alpha q_e}{q_{mFG}}}}$ | [61] |
| Moreau | 3 | $q_e = q_{mM} \frac{b C_e + l b^2 C_e^2}{1 + 2b C_e + l b^2 C_e^2}$ | [62] |
| Unilan | 3 | $q_e = \frac{q_{mU}}{2b_U} \ln \left(\frac{a_U + C_e e^{b_U}}{a_U + C_e e^{-b_U}} \right)$ | |

Note *Implicit equation or function.

Application of Multiobjective Optimization by Ratio Analysis (MOORA) in Modeling

The Multiobjective Optimization by Ratio Analysis (MOORA) was employed for multi-criteria decision-making (MCDM) in the modeling exercise since a mixture of error function superiority is often found for the top models. This approach facilitates the selection of the optimal model by simultaneously evaluating multiple performance metrics [26,27]. The methodology consists of the 1st step of the normalization of the decision matrix to ensure comparability among different performance metrics; the decision matrix was normalized. Given that these metrics may have varying units and magnitudes, normalization needs to be carried out using the following equation:

$$X'_{ij} = \frac{X_{ij}}{\sqrt{\sum_{i=1}^n X_{ij}^2}} \quad (\text{Eqn. 10})$$

Where X_{ij} is the original value of the j^{th} metric for the i^{th} model, and X'_{ij} is the normalized value.

Ratio System Analysis

The normalized values were then aggregated using an approach of a ratio system. Beneficial criteria (those that should be maximized, $adjR^2$) were summed up, while non-beneficial criteria (the rest of the error functions) or those that should be minimized were subtracted using the following formula:

$$Y_i = \sum_{\text{beneficial}} X'_{ij} - \sum_{\text{non-beneficial}} X'_{ij} \quad (\text{Eqn. 11})$$

Where Y_i is the final score for the i^{th} model

In circumstances where certain criteria were deemed more crucial than others, weighted ratios are recommended to be incorporated into the analysis. The suggestion for incorporating Weighted Ratios is not carried out at this point in time as the consensus for which error functions listed above has priority over the other has not been documented in the literature. The final step is ranking models based on their aggregated performance scores. Higher scores indicated superior performance. The model with the highest value was considered the most optimal based on the given decision criteria. This methodology allowed for an objective and systematic comparison of kinetic models, facilitating the identification of the best-performing model while considering multiple performance metrics simultaneously.

RESULTS AND DISCUSSION

Several models were applied to the equilibrium data of [32] by nonlinear regression. Notably, as shown in **Figs. 1-18**, all of these models showed good data fits with the exception of the Henry and the Dubinin-Radushkevich model, of which the latter failed to converge. The error function analysis is shown in **Table 2**. The Multiobjective Optimization on the Basis of Ratio Analysis (MOORA) approach was used to compare the adsorption isotherm models' effectiveness, which is presented in **Table 3**. The top five models in descending order were found to be the Koble-Corrigan, Brouers-Sotolongo, Fritz-Schlunder III, Hill, and Sips models ranked in the form of the SCO or the Standard Competition Order (1-2-2-4), where when two ranks are tied, they received the same rank and the next rank will be skipped one rank. MOORA's uses the SCO as the basis of ranking and its uses in academia as a rank system is reported early in the year 2009 [65] based on a Google Scholar search for the term "Standard Competition Order" 1-2-2-4 rule.

The compared isotherms were found to show higher fitting capability than other evaluated isotherms. These models were then compared with the Langmuir and Freundlich models. The Langmuir, Brouers-Sotolongo, Sips, and Hill models were able to estimate the maximum adsorption capacity (q_m) with relatively narrow confidence intervals. Conversely, the Langmuir model exhibited a wide confidence interval (Table 4), which may indicate a lower precision in the estimation. However, the Fritz-Schlunder-III model was found to overestimate the q_m significantly and gave a very high value. This inconsistency may be due to the model being overfitted, or the model might not have been able to properly capture the adsorption equilibrium data within the range of concentrations used in the study. Nevertheless, the Freundlich, Koble-Corrigan, and Brouers-Sotolongo models were found to be unable to estimate the q_m because they are more empirical or semi-empirical models which are often used to describe the adsorption process rather than estimating the saturation capacity.

Out of the models assessed, the Brouers-Sotolongo isotherm was found to be the most accurate model for determining q_m . This conclusion is drawn from the fact that it can produce a precise estimate with narrow confidence limits while taking into consideration the heterogeneity of the adsorption process. The Langmuir model, nevertheless, remains popular despite a higher level of uncertainty in its application.

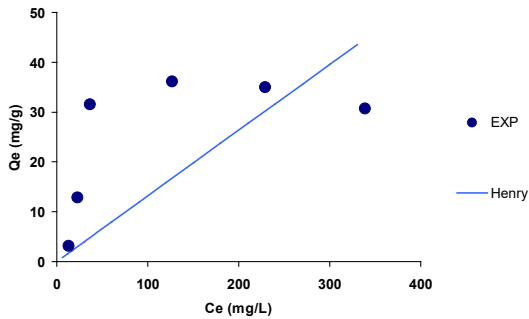


Fig. 1. Copper adsorption onto chitosan-silica composite aerogel modelled using the Henry model.

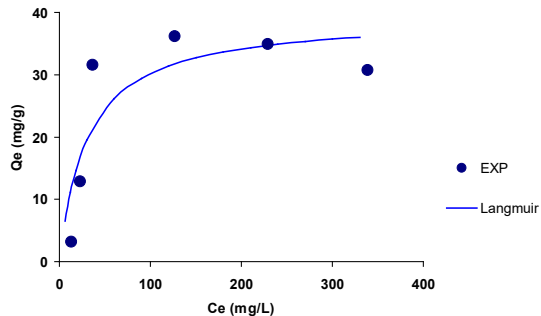


Fig. 2. Copper adsorption onto chitosan-silica composite aerogel modelled using the Langmuir isotherm model.

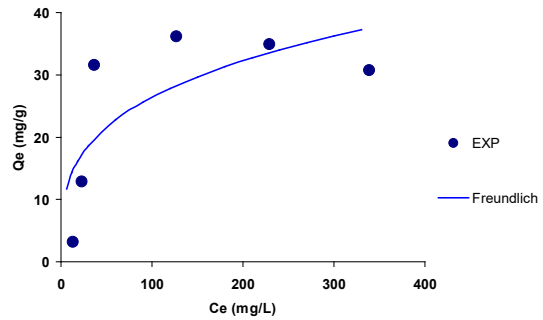


Fig. 3. Copper adsorption onto chitosan-silica composite aerogel modelled using the Freundlich isotherm model.

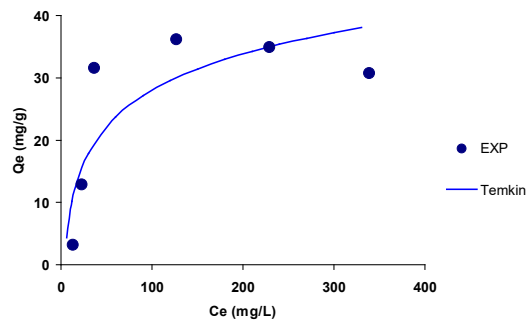


Fig. 4. Copper adsorption onto chitosan-silica composite aerogel modelled using the Temkin isotherm model.

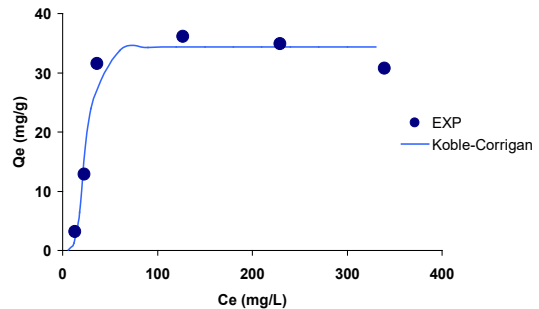


Fig. 5. Copper adsorption onto chitosan-silica composite aerogel modelled using the Koble-Corrigan isotherm model.

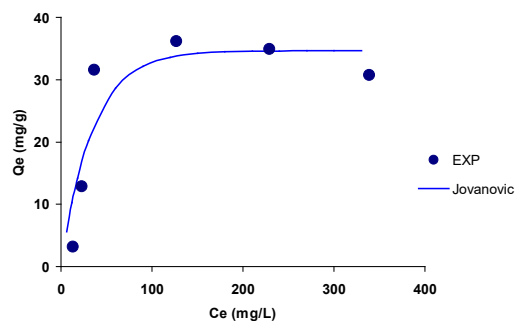


Fig. 6. Copper adsorption onto chitosan-silica composite aerogel modelled using the Jovanovic isotherm model.

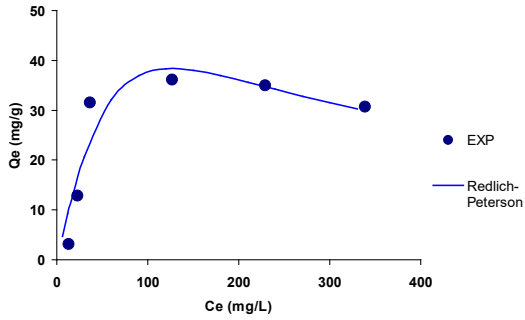


Fig. 7. Copper adsorption onto chitosan-silica composite aerogel modelled using the Redlich-Peterson isotherm model.

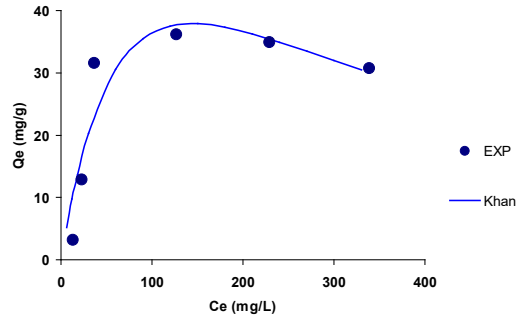


Fig. 11. Copper adsorption onto chitosan-silica composite aerogel modelled using the Khan isotherm model.

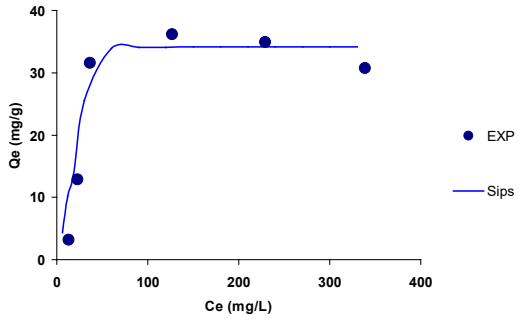


Fig. 8. Copper adsorption onto chitosan-silica composite aerogel modelled using the Sips isotherm model.

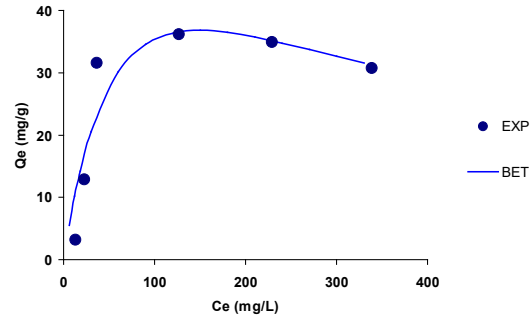


Fig. 12. Copper adsorption onto chitosan-silica composite aerogel modelled using the BET isotherm model.

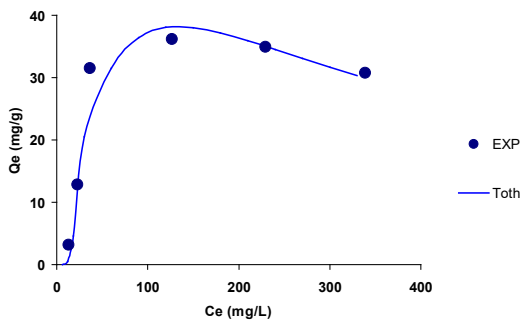


Fig. 9. Copper adsorption onto chitosan-silica composite aerogel modelled using the Toth isotherm model.

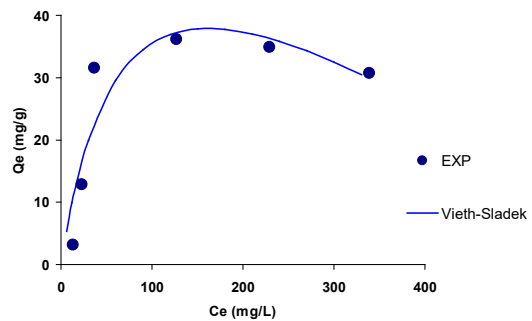


Fig. 13. Copper adsorption onto chitosan-silica composite aerogel modelled using the Vieth-Sladek isotherm model.

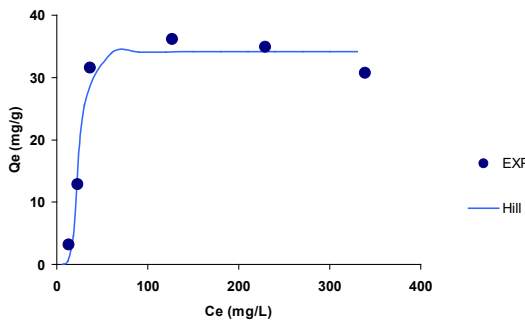


Fig. 10. Copper adsorption onto chitosan-silica composite aerogel modelled using the Hill isotherm model.

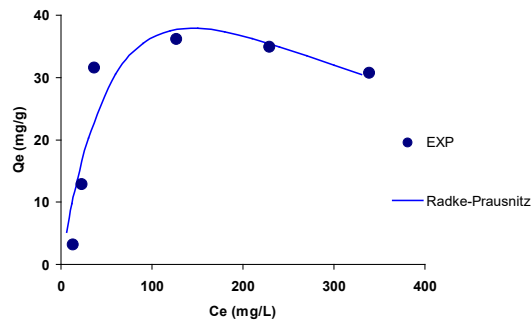


Fig. 14. Copper adsorption onto chitosan-silica composite aerogel modelled using the Radke-Prausnitz isotherm model.

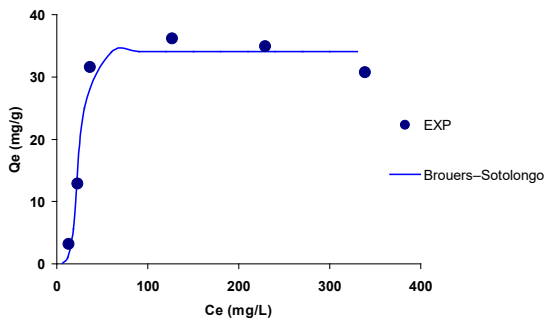


Fig. 15. Copper adsorption onto chitosan–silica composite aerogel modelled using the Brouers-Sotolongo isotherm model.

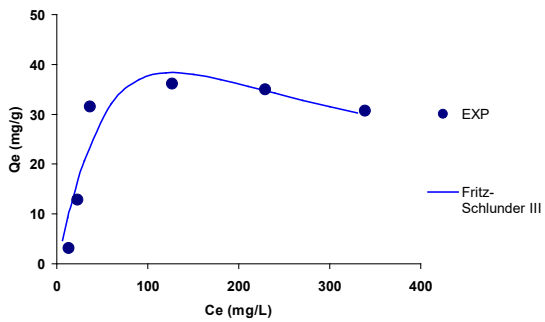


Fig. 16. Copper adsorption onto chitosan–silica composite aerogel modelled using the Fritz-Schlunder III isotherm model.

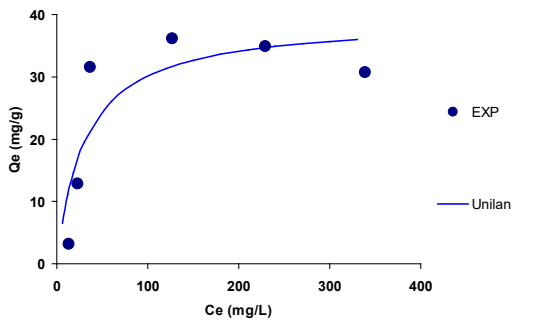


Fig. 17. Copper adsorption onto chitosan–silica composite aerogel modelled using the Unilan isotherm model.

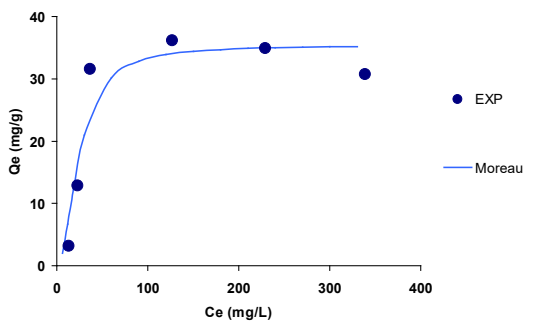


Fig. 18. Copper adsorption onto chitosan–silica composite aerogel modelled using the Moreau isotherm model.

Table 2. Error function analysis for the fitting of the isotherm of copper adsorption onto chitosan–silica composite aerogel.

| Model | <i>p</i> | MPSD | RMSE | <i>adrR</i> ² | AICc | BIC | HQC | BF | AF |
|---------------------|----------|--------|--------|--------------------------|--------|-------|-------|-------|-------|
| Henry | 1 | 1678.6 | 16.786 | -0.157 | 42.753 | 34.54 | 33.92 | 0.525 | 2.157 |
| Langmuir | 2 | 776.7 | 7.767 | 0.217 | 44.167 | 25.75 | 24.50 | 0.986 | 1.174 |
| Freundlich | 2 | 1002.3 | 10.023 | -0.539 | 47.226 | 28.81 | 27.56 | 0.958 | 1.232 |
| Temkin | 3 | 1010.2 | 10.102 | -0.240 | 77.594 | 28.97 | 27.09 | 0.960 | 1.198 |
| Koble-Corrigan | 2 | 249.72 | 2.497 | 0.96 | 30.549 | 12.13 | 10.88 | 0.901 | 1.059 |
| Jovanovic | 2 | 664.17 | 6.642 | 0.442 | 42.288 | 23.87 | 22.62 | 0.999 | 1.143 |
| Redlich-Peterson | 3 | 644.33 | 6.443 | 0.473 | 72.198 | 23.57 | 21.70 | 1.001 | 1.110 |
| Sips | 3 | 275.28 | 2.753 | 0.943 | 61.993 | 13.37 | 11.49 | 1.006 | 1.042 |
| Toth | 3 | 661.24 | 6.612 | 0.443 | 72.509 | 23.88 | 22.01 | 0.999 | 1.111 |
| Hill | 3 | 275.28 | 2.753 | 0.943 | 61.993 | 13.37 | 11.49 | 1.006 | 1.042 |
| Khan | 3 | 687.88 | 6.879 | 0.386 | 72.982 | 24.36 | 22.48 | 0.997 | 1.115 |
| BET | 3 | 697.74 | 6.977 | 0.321 | 73.153 | 24.53 | 22.65 | 1.002 | 1.109 |
| Vieth-Sladek | 3 | 713.44 | 7.134 | 0.346 | 73.420 | 24.80 | 22.92 | 0.993 | 1.121 |
| Radke-Prausnitz | 3 | 687.88 | 6.879 | 0.386 | 72.982 | 24.36 | 22.48 | 0.997 | 1.115 |
| Brouers-Sotolongo | 3 | 258.08 | 2.581 | 0.948 | 61.218 | 12.59 | 10.72 | 1.007 | 1.043 |
| Fritz-Schlunder III | 3 | 258.08 | 2.581 | 0.948 | 61.218 | 12.59 | 10.72 | 1.007 | 1.043 |
| Unilan | 3 | 897.25 | 8.972 | -0.177 | 76.171 | 27.55 | 25.67 | 0.985 | 1.174 |
| Fowler-Guggenheim | 3 | 316.29 | 3.163 | 0.926 | 63.659 | 15.03 | 13.16 | 0.994 | 0.994 |
| Moreau | 3 | 607.54 | 6.075 | 0.581 | 71.492 | 22.87 | 20.99 | 1.008 | 1.008 |

Note:
 RMSE Root mean Square Error
*adrR*² Adjusted Coefficient of determination
p no of parameters
 AF Accuracy factor
 BF Bias factor
 BIC Bayesian Information Criterion
 AICc Adjusted Akaike Information Criterion
 HQC Hannan–Quinn information criterion

Table 3. Ranking of isothermal models based on MOORA.

| Model | MOORA's Ratio value | Rank |
|---------------------|---------------------|------|
| Koble-Corrigan | -6.37 | 1 |
| Brouers-Sotolongo | -16.60 | 2 |
| Fritz-Schlunder III | -16.60 | 2 |
| Hill | -17.36 | 4 |
| Sips | -17.36 | 4 |
| Jovanovic | -18.98 | 6 |
| Fowler-Guggenheim | -19.10 | 7 |
| Langmuir | -21.95 | 8 |
| Freundlich | -27.77 | 9 |
| Moreau | -29.50 | 10 |
| Redlich-Peterson | -30.64 | 11 |
| Toth | -31.16 | 12 |
| Radke-Prausnitz | -31.97 | 13 |
| Khan | -31.97 | 13 |
| BET | -32.26 | 15 |
| Vieth-Sladek | -32.73 | 16 |
| Unilan | -38.07 | 17 |
| Henry | -40.68 | 18 |
| Temkin | -41.16 | 19 |

Koble-Corrigan, Hill, and Sips models

The Koble-Corrigan isotherm model is a 3-parameter adsorption model. The model combines the features of Langmuir and Freundlich models to fit data from heterogeneous surfaces with different energy sites. Since this model can designate both monolayer and multilayer adsorption, it is useful when the Freundlich model fits the data poorly at high surface site capacities, and the Langmuir model fits the data poorly at low surface site capacities. This model is used extensively in environmental and industrial adsorption studies in wastewater treatment, heavy metal removal, and dye adsorption [66–68]. It has an exponent parameter that better describes various systems' adsorption intensity and capacity. As a result, estimating model parameters is a nonlinear regression task, which is more time-consuming than other simpler isotherm models. Nevertheless, its complexity is rewarded with a more realistic description of the adsorption behaviour on real-world heterogeneous adsorbents, which makes it a valuable tool in adsorption science and engineering.

Table 4: Isothermal models' constants for copper adsorption onto chitosan–silica composite aerogel .

| Model | p | Unit | Value | (95% confidence interval) |
|---------------------------------------|-------------------------|--|--|---------------------------------|
| Langmuir | q_{mL} | mg g ⁻¹ | 39.329 | 19.273 to 59.387 |
| | b_L | L mg ⁻¹ | 0.0328 | -0.0293 to 0.0951 |
| Freundlich [#] | K_F | (mg g ⁻¹ ·L mg ⁻¹) ^{1/n} | 6.996 | -8.124 to 22.117 |
| | n_F | (¹) | 3.467 | -1.650 to 8.584 |
| Koble-Corrigan [#] | A | (mg g ⁻¹)(L mg ⁻¹) ⁿ | 0.000017288 | -0.00024 to 0.00028 |
| | B | (L mg ⁻¹) ⁿ | 0.0000005027 | -0.000007 to 0.000008 |
| | n | dimensionless | 4.51 | -0.155 to 9.174 |
| Koble-Corrigan (test for equivalence) | for A/B $=q_{mKC}$ | mg g ⁻¹ | 34.3902924 (8 decimal points for values of A and B) 17.000 (6 decimal points for values of A and B) | |
| Brouers-Sotolongo | q_{mBS} | mg g ⁻¹ | 34.01 | 29.605 to 38.410 |
| | K_{BS} | mg ^{1/nBS} L ^{1/nBS} | 0.00009 | -0.00006 to 0.00008 |
| | n_{BS} | dimensionless | 0.29 | 0.073 to 0.498 |
| Sips | q_{mS} | mg g ⁻¹ | <u>34.114</u> | 29.089 to 39.139 |
| | K_S | (L mg ⁻¹) ^{ns} | 0.000000008504 | -0.0000001 to 0.0000002 |
| | n_S | dimensionless | 0.172861 | -0.0302 to 0.376 |
| Sips (test for equivalence) | $1/n_S$ $1/K_S$ | L ⁻ⁿ mg ⁿ | <u>5.78489</u> <u>117557243.87</u> | |
| Hill | q_{mH} | mg g ⁻¹ | <u>34.114</u> | 29.09 to 39.14 |
| | n_H | dimensionless | <u>5.78489</u> | -1.01 to 12.58 |
| | K_H | mg L ⁻¹ | <u>117557243.87</u> | -2412930516.71 to 2648045004.45 |
| Fritz-Schlunder-III | q_{mFS} | mg g ⁻¹ | 1217.68 | -8572.67 to 11008.04 |
| | K_{FS} | L mg ⁻¹ | 0.00066 | -0.00513 to 0.00644 |
| | n_{FS} | dimensionless | 1.616 | 0.173 to 3.058 |

Note

[#]Isotherms that have no direct way in estimating maximum adsorption capacity (mg g⁻¹). Underlined values indicate the same values shared by more than one model.

The Sips model integrates the highly utilized Langmuir and Freundlich isotherms and facilitates the prediction of heterogeneous adsorption systems. The Sips model addresses the limitations encountered in modeling elevated solute concentrations inherent to the Freundlich model. At low solute concentrations, it effectively converges to the Freundlich isotherm. At high solute concentrations, it simplifies the Langmuir model of monolayer sorption capacity [69]. The Sips model is found to be the best model in various sorption studies [70–75].

The Hill model was introduced and is based on the notion of a mobile-first layer conforming to a two-dimensional van der Waals equation. Nonetheless, the Hill model was found to be the most effective in scenarios involving moderately elevated concentrations. It points towards the strength of attraction between an adsorbent and its intended adsorbates, which is demonstrated by the steepening of the isotherm curves at increasing values of K_H . By modifying the values of n_H , a range of isotherms can be deduced from the Hill model, which encompasses the S- and L-shaped curves. Chu et al. [76] recently demonstrated the mathematical equivalence of the Hill, Liu, Sips, and Koble–Corrigan isotherm models. However, to sustain these models' historical context and original conceptual individualisms, they will continue to be depicted in their traditional forms to preserve each of the model's theoretical interpretations while acknowledging their underlying similarities. An interesting observation regarding the MOORA's ranking is that the Koble-Corrigan model is given the first rank whilst both the Sips and Hill model, each receive a rank of 2, confirming their mathematical equivalence as shown by Chu [76] and also demonstrated in the same values for the parameters in the (test for equivalence) row. The question is why does the Koble-Corrigan model does not receive the same rank? The analysis presented in **Table 4** for the Koble-Corrigan model (test for equivalence) suggests that the observed discrepancy is likely due to the sensitivity of the calculated parameter values to the number of decimal places used in the computation. In certain datasets, such as the one used by Chu, the parameter q_m is derived

from the division of A by B (or A/B). In Chu et al., [76] these parameters are denoted as Q and b_K , respectively, leading to a calculated value of $q_m=17.88/0.006=2980$ $q_m= 17.88/0.006 = 2980$ mg/g.

In **Table 3** of Chu's paper, the calculated q_m value for the Sips, Liu, and Hill models was consistently reported as 2795 mg/g. If the Koble-Corrigan model were to be considered mathematically equivalent to the Sips, Liu, and Hill models, the q_m value should align accordingly. Additionally, the dimensionless parameter n was reported as 0.748 for the Koble-Corrigan, Sips, Liu, and Hill models [76]. Given this equivalency, the other parameters should be determinable with precision, except for q_m , which appears inconsistent. This discrepancy is likely due to the number of decimal places used in calculations for the Koble-Corrigan model. While it is mathematically equivalent to the Sips, Liu, and Hill models, the exact parameter values may differ slightly due to rounding and numerical precision in the computation process.

Fritz-Schlunder III

The Fritz Schlunder III isotherm is a model employed to explain the adsorption processes on surfaces having varying characteristics. It integrates the elements of the Langmuir and Freundlich isotherms, which renders it suitable for certain situations where adsorption sites display differences in energy levels and capacities. This model demonstrated significant efficacies in real-world data for limited adsorption systems. Its advantage is its ability to accommodate adsorption energies and capacities, and it is a valuable model for the prediction of the adsorption process in heterogeneous systems [60].

Brouers-Sotolongo

The Brouers-Sotolongo (BS) model is an isotherm model whose development incorporates the principles of the classical models to describe the adsorption processes on heterogeneous surfaces. The BS model was developed by incorporating new parameters representing the variety and complexity of active sites on the adsorbent material. The BS model provides a generalised

approach to the description of adsorption isotherms. The superiority of the model has been shown in numerous applications.

The BS model was found to be the best fit for the adsorption data in a study that involved the biosorption of Yellow Tartrazine dye using the agro-industrial wastes sugarcane bagasse and rice husk [77]. Another investigation for metal sorption on soils that utilizes models including Brouers-Sotolongo, Sips, Hill, and Langmuir-Freundlich models showed that the BS model fitted the experimental data very well [78]. More recent work on the adsorption of mercury (II) ions (Hg^{2+}) onto a novel porous organic polymer also showed the BS as the best model [79]. Another work on removing Gram negative enteric bacteria using a hybrid clay composite that is surface-modified with chitosan also showed the BS model as the best model [80].

MOORA distinguishes itself through its simplicity and computational efficiency, as it normalizes performance ratings across criteria, eliminating the need for complex pairwise comparisons or distance calculations. This approach is particularly advantageous when handling criteria with different units and scales, allowing for transparent and rapid evaluation. Although MCDM has been extensively applied in other model ranking exercises, such as evaluating Software Reliability Growth Models (SRGMs) [81], its application in adsorption model selection remains scarce. A significant limitation of nonlinear modeling is that small datasets (such as the six data points used in this study) may fail to adequately describe adsorption behavior. Limited data increases the likelihood of capturing random noise rather than true adsorption trends, leading to overfitting and unreliable parameter estimation. Small datasets also suffer from low statistical power, wider confidence intervals, and difficulty in model validation. To mitigate these challenges, statistical techniques such as Monte Carlo simulations, bootstrapping, and sensitivity analysis can improve model robustness and provide deeper insight into adsorption behavior [82].

In the original publication of [32], the values obtained in this study are similar, but the Langmuir choice as the better model based on AIN and BIC is premature as the difference in values is less than 5. In addition, extracted residual data for the sum of squared residuals (SSR) of the Hill model was 30.56, while for the Langmuir model, it was 266.26, suggesting a better fit for the Hill model. Since the Freundlich model was not shown in Figure 4b despite the fitting parameter values are shown in **Table 4** of [32], it was excluded from the analysis. Additionally, the coefficient of determination (R^2) calculated by us for the extracted data for the Hill model was 0.9787, meaning it describes 97.87% of the variance in the experimental data, whereas, for the Langmuir model, it was 81.42% ($R^2 = 0.8142$). Even when accounting for model complexity using the adjusted R^2 that penalizes for the extra parameter of the Hill's model, the Hill model remains superior, with an adjusted R^2 of 0.9573 compared to 0.7213 for the Langmuir model based on our calculations. These results uphold that the Hill model provides a significantly better representation of the adsorption activity, establishing it as the preferred model in contrast to the original findings of [32]. The R^2 value is reported for the Weber and Morris model but missing from the pseudo-first-order and pseudo-second-order models in **Table 3** [32]. As R^2 is one of the most popular goodness-of-fit metrics, the lack of it makes it very difficult to justify why the pseudo-second-order model is better than the others. This inconsistency is further compounded by the isothermal model fitting where no R^2 values are reported for Figure 4b of [32], even though it was initially utilized to choose

the best kinetics model. Since the comparison of models involves different parameters, the adjusted R^2 should have been used instead because it penalizes the number of parameters. We demonstrated that even using adjusted R^2 , the Hill model is still the best compared to Langmuir. Without this correction, the preference of one model over the other may be misleading because of overfitting. Further, the application of AIC and BIC is not thorough because the authors do not present the delta values of AIC and BIC as Motulsky and Ranas (2006) recommended. As pointed out by statistical best practices, a $\Delta\text{AIC} > 5$ is required to establish the difference between models firmly.

This paper [32] shows that the reported AIC and BIC values show only small differences; hence, the conclusions based on these criteria may not be statistically significant. Thus, the lack of a correct assessment of ΔAIC and ΔBIC makes it doubtful to choose the best kinetic and isotherm models. Our application of MOORA demonstrated superior performance in ranking adsorption models, overcoming the inconsistencies of previous analyses. The original conclusions by Vareda et al. [32] can be strengthened by incorporating additional error functions and a structured MCDM approach, reinforcing the reliability of adsorption model selection.

CONCLUSION

The equilibrium adsorption data from a published work were reanalyzed using several nonlinear regression models, and it was found that most of the models fitted the data well except for the Henry and Dubinin-Radushkevich models. The Multiobjective Optimization on the Basis of Ratio Analysis (MOORA) was applied to develop a systematic or objective approach for ranking the adsorption isotherms, and the ranking result showed that the order of isotherms is Koble-Corrigan, Brouers-Sotolongo, Fritz-Schlunder III, Hill and Sips. The Brouers-Sotolongo model was discovered to be the most accurate in the estimation of maximum adsorption capacity (q_m) because it could incorporate the phenomenon of surface heterogeneity while maintaining accuracy with narrow confidence intervals. These results show that the Langmuir model is not without its limitations; even though it is one of the most popular models, it has a wide confidence interval and low precision. Furthermore, the Fritz-Schlunder III model was discovered to overestimate q_m significantly, which may be attributed to overfitting. It was thus possible to establish that the Koble-Corrigan, Sips, Hill, and Liu models are equivalent mathematically, but the slight disagreements in the calculated parameter values were accredited to rounding of the decimal points. The main weakness of this and many isothermal studies was the size of the dataset which can affect the accuracy of the model fitting and possible mechanistic interpretation of adsorption processes. In order to address this, it is suggested that in future work, more data should be collected and analyzed, and statistical procedures such as Monte Carlo simulations and bootstrapping should be used to increase the stability of the models. Furthermore, the result of this study stresses the importance of using statistical criteria, such as adjusted R^2 and $\Delta\text{AIC}/\text{BIC}$, for model identification and to use and report them nonselectively. The use of MOORA in the ranking of adsorption models has been found to be a better and more systematic way of making the analysis than what has been done previously. These results support the previous findings, which suggest that it is necessary to employ multiple evaluation criteria for the adsorption systems in order to gain a fuller understanding of the adsorption processes.

REFERENCES

- Shukor MY. Outlier and Normality Testing of the Residuals from the Carreau-Yasuda Model in Fitting the Rheological Behavior of the Non-Newtonian fluid TF2N. *Bioremediation Sci Technol Res.* 2021 Jul 31;9(1):20–6.
- Shukor MY. Bartlett and the Levene's tests of homoscedasticity of the modified Gompertz model used in fitting of *Burkholderia* sp. strain Neni-11 growth on acrylamide. *Bioremediation Sci Technol Res.* 2016 Jul 31;4(1):18–9.
- Huitema BE, McKean JW, Zhao J. The runs test for autocorrelated errors: unacceptable properties. *J Educ Behav Stat.* 1996;21(4):390–404.
- Foo KY, Hameed BH. Insights into the modeling of adsorption isotherm systems. *Chem Eng J.* 2010;156(1):2–10.
- Wang Y, Wang C, Huang X, Zhang Q, Wang T, Guo X. Guideline for modeling solid-liquid adsorption: Kinetics, isotherm, fixed bed, and thermodynamics. *Chemosphere.* 2024 Feb 1;349:140736.
- Ezekiel M. The Sampling Variability of Linear and Curvilinear Regressions: A First Approximation to the Reliability of the Results Secured by the Graphic "Successive Approximation" Method. *Ann Math Stat.* 1930;1(4):275–333.
- Akaike H. A New Look at the Statistical Model Identification. *IEEE Trans Autom Control.* 1974;19(6):716–23.
- Burnham KP, Anderson DR. Multimodel inference: Understanding AIC and BIC in model selection. *Sociol Methods Res.* 2004;33(2):261–304.
- Schwarz G. Estimating the Dimension of a Model. *Ann Stat.* 1978;6(2):461–4.
- Hannan EJ, Quinn BG. The Determination of the Order of an Autoregression. *J R Stat Soc Ser B Methodol.* 1979;41(2):190–5.
- Marquardt DW. An Algorithm for Least-Squares Estimation of Nonlinear Parameters. *J Soc Ind Appl Math.* 1963;11(2):431–41.
- Seidel A, Gelbin D. On applying the ideal adsorbed solution theory to multicomponent adsorption equilibria of dissolved organic components on activated carbon. *Chem Eng Sci.* 1988 Jan 1;43(1):79–88.
- Porter JF, McKay G, Choy KH. The prediction of sorption from a binary mixture of acidic dyes using single- and mixed-isotherm variants of the ideal adsorbed solute theory. *Chem Eng Sci.* 1999;54(24):5863–85.
- Vilardi G, Di Palma L, Verdona N. Heavy metals adsorption by banana peels micro-powder: Equilibrium modeling by nonlinear models. *Chin J Chem Eng.* 2018 Mar 1;26(3):455–64.
- Manjunatha CR, Nagabhushana BM, Naryana A, Usha P, Raghu MS, Adrsha JR. Adsorption of fluoride and DB-53 dye onto PLA/rGO nanoparticles: Mathematical modeling and statistical studies. *J Water Process Eng.* 2021 Dec 1;44:102447.
- Asha PK, Deepak K, Prashanth MK, Parashuram L, Devi VSA, Archana S, et al. Ag decorated Zn-Al layered double hydroxide for adsorptive removal of heavy metals and antimicrobial activity: Numerical investigations, statistical analysis and kinetic studies. *Environ Nanotechnol Monit Manag.* 2023 Dec 1;20:100787.
- Khayat ME, Shukor MY. A Fixed-Bed Study on the Feedsorption of BSA Using PKC: Toward the Sustainable Agrisorption of Protein-rich Waste for Enhancing Low Nutritional-value Feed. *Bioremediation Sci Technol Res E-ISSN 2289-5892.* 2023 Dec 31;11(2):1–9.
- Saaty TL. *The Analytic Hierarchy Process: Planning, Priority Setting, Resource Allocation.* New York: McGraw-Hill; 1980. 287 p.
- Hwang CL, Yoon K. *Multiple Attribute Decision Making: Methods and Applications A State-of-the-Art Survey.* 1st edition. Berlin Heidelberg: Springer; 1981. 280 p.
- Brans JP. L'ingénierie de la décision; élaboration d'instruments d'aide à la décision. La méthode PROMETHEE [Decision engineering; development of decision support tools. The PROMETHEE method]. In: Nadeau R, Landry M, editors. *L'aide à la décision: nature, instruments et perspectives d'avenir.* Québec, Canada: Presses de l'Université Laval; 1982. p. 183-213.
- Fishburn PC. Additive Utilities with Incomplete Product Sets: Application to Priorities and Assignments. *Oper Res.* 1967 May 1;15:537.
- Triantaphyllou E. *Multi-criteria Decision Making Methods: A Comparative Study.* 2000th edition. Dordrecht: Springer; 2000. 320 p.
- Hamurcu M, Eren T. Applications of the MOORA and TOPSIS methods for decision of electric vehicles in public transportation technology. *Transport.* 2022 Nov 18;37:251–63.
- Homayounfar M, Fadaei M, Gheibodoust H, Rezaee Kelidbari H. A Systematic Literature Review on MOORA Methodologies and Applications. *Iran J Oper Res.* 2022 Jan 1;13:164–83.
- Brauers WK. Multiobjective optimization (moo) in privatization. *J Bus Econ Manag.* 2004 Jan 1;5(2):59–65.
- Brauers W. Multi-objective seaport planning by MOORA decision making. *Ann Oper Res.* 2013 Jul 1;206.
- Karel W, Brauers W, Zavadskas E. The MOORA method and its application to privatization in a transition economy. *Control Cybern.* 2006 Jan 1;35.
- Rahim R, Siahaan APU, Farta Wijaya R, Hantono H, Aswan N, Thamrin S, et al. Technique for Order of Preference by Similarity to Ideal Solution (TOPSIS) method for decision support system in top management. *Int J Eng Technol.* 2018 Jan 1;7:290–3.
- Barik T, Parida S, Pal K. Optimizing Process Parameters in Drilling of CFRP Laminates: A Combined MOORA–TOPSIS–VIKOR Approach. *Fibers Polym.* 2024 May 1;25(5):1859–76.
- Turan E, Özkan A. Prioritization of amine-based solid sorbents for post-combustion CO₂ capture using different multi-criteria decision-making tools. *Int J Environ Sci Technol [Internet].* 2024 Dec 16 [cited 2025 Feb 17]; Available from: <https://doi.org/10.1007/s13762-024-06181-8>
- Azari A, Nabizadeh R, Mahvi AH, Nasserli S. Integrated Fuzzy AHP-TOPSIS for selecting the best color removal process using carbon-based adsorbent materials: multi-criteria decision making vs. systematic review approaches and modeling of textile wastewater treatment in real conditions. *Int J Environ Anal Chem.* 2022 Dec 28;102(18):7329–44.
- Varela JP, Matias PMC, Paixão JA, Murtinho D, Valente AJM, Durães L. Chitosan–Silica Composite Aerogel for the Adsorption of Cupric Ions. *Gels.* 2024 Mar;10(3):192.
- Tawfik GM, Dila KAS, Mohamed MYF, Tam DNH, Kien ND, Ahmed AM, et al. A step by step guide for conducting a systematic review and meta-analysis with simulation data. *Trop Med Health.* 2019 Aug 1;47(1):46.
- Khare KS, Phelan FR. Quantitative Comparison of Atomistic Simulations with Experiment for a Cross-Linked Epoxy: A Specific Volume-Cooling Rate Analysis. *Macromolecules.* 2018;51(2):564–75.
- Langmuir I. THE ADSORPTION OF GASES ON PLANE SURFACES OF GLASS, MICA AND PLATINUM. *J Am Chem Soc.* 1918;40(2):1361–402.
- Schirmer W. Physical Chemistry of Surfaces. *Z Für Phys Chem.* 1999;210(1):134–5.
- Ridha FN, Webley PA. Anomalous Henry's law behavior of nitrogen and carbon dioxide adsorption on alkali-exchanged chabazite zeolites. *Sep Purif Technol.* 2009;67(3):336–43.
- Jovanović DS. Physical adsorption of gases - I: Isotherms for monolayer and multilayer adsorption. *Kolloid-Z Amp Z Für Polym.* 1969;235(1):1203–13.
- Carmo AM, Hundal LS, Thompson ML. Sorption of hydrophobic organic compounds by soil materials: Application of unit equivalent Freundlich coefficients. *Environ Sci Technol.* 2000;34(20):4363–9.
- Radushkevich LV. Potential theory of sorption and structure of carbons. *Zhurnal Fiz Khimii.* 1949;23:1410–20.
- Dubinin MM. Modern state of the theory of volume filling of micropore adsorbents during adsorption of gases and steams on carbon adsorbents. *Zh Fiz Khim.* 1965;39(6):1305–17.
- Mahanty B, Behera SK, Sahoo NK. Misinterpretation of Dubinin–Radushkevich isotherm and its implications on adsorption parameter estimates. *Sep Sci Technol.* 2023 May 3;58(7):1275–82.
- Mudhoo A, Pittman CU. The Dubinin-Radushkevich models: Dissecting the *ps/p* to *cs/ce* replacement in solid-aqueous interfacial adsorption and tracking the validity of $E = 8 \text{ kJ mol}^{-1}$ for assigning sorption type. *Chem Eng Res Des.* 2023 Oct 1;198:370–402.
- Koble RA, Corrigan TE. Adsorption isotherms for pure hydrocarbons. *Ind Eng Chem.* 1952 Feb 1;44(2):383–7.
- Temkin MI, Pyzhev V. Kinetics of ammonia synthesis on promoted iron catalysts. *Acta Physicochim USSR.* 1940;12(3):327–56.

46. Chu KH. Revisiting the Temkin Isotherm: Dimensional Inconsistency and Approximate Forms. *Ind Eng Chem Res* [Internet]. 2021 Aug 16 [cited 2022 Sep 1]; Available from: <https://pubs.acs.org/doi/pdf/10.1021/acs.iecr.1c01788>
47. Redlich O, Peterson DL. A Useful Adsorption Isotherm. *Shell Dev Co Emeryv Calif*. 1958;63:1024.
48. Sips R. On the structure of a catalyst surface. *J Chem Phys*. 1948;16(5):490–5.
49. Tóth J. Uniform interpretation of gas/solid adsorption. *Adv Colloid Interface Sci*. 1995;55(C):1–239.
50. Hill AV. The possible effects of the aggregation of the molecules of haemoglobin on its dissociation curves. *J Physiol*. 1910;40:iv–vii.
51. Khan AA, Singh RP. Adsorption thermodynamics of carbofuran on Sn (IV) arsenosilicate in H⁺, Na⁺ and Ca²⁺ forms. *Colloids Surf*. 1987;24(1):33–42.
52. Brunauer S, Emmett PH, Teller E. Adsorption of Gases in Multimolecular Layers. *J Am Chem Soc*. 1938;60(2):309–19.
53. Vieth WR, Sladek KJ. A model for diffusion in a glassy polymer. *J Colloid Sci*. 1965;20(9):1014–33.
54. Radke CJ, Prausnitz JM. Adsorption of Organic Solutes from Dilute Aqueous Solution of Activated Carbon. *J Am Chem Soc*. 1972;11(4):445–51.
55. Liu Y, Liu YJ. Biosorption isotherms, kinetics and thermodynamics. *Sep Purif Technol*. 2008;61(3):229–42.
56. Tran HN, Bollinger JC, Lima EC, Juang RS. How to avoid mistakes in treating adsorption isotherm data (liquid and solid phases): Some comments about correctly using Radke-Prausnitz nonlinear model and Langmuir equilibrium constant. *J Environ Manage*. 2023 Jan 1;325(Pt A):116475.
57. Brouers F, Sotolongo O, Marquez F, Pirard JP. Microporous and heterogeneous surface adsorption isotherms arising from Levy distributions. *Phys Stat Mech Its Appl*. 2005 Apr 1;349(1):271–82.
58. Hamissa AMB, Brouers F, Mahjoub B, Seffen M. Adsorption of Textile Dyes Using Agave Americana (L.) Fibres: Equilibrium and Kinetics Modelling. *Adsorpt Sci Technol*. 2007 Jun 1;25(5):311–25.
59. Brouers F, Al-Musawi TJ. Brouers-Sotolongo fractal kinetics versus fractional derivative kinetics: A new strategy to analyze the pollutants sorption kinetics in porous materials. *J Hazard Mater*. 2018 May 15;350:162–8.
60. Fritz W, Schlueder EU. Simultaneous adsorption equilibria of organic solutes in dilute aqueous solutions on activated carbon. *Chem Eng Sci*. 1974;29(5):1279–82.
61. Chu KH, Tan B. Is the Frumkin (Fowler–Guggenheim) adsorption isotherm a two- or three-parameter equation? *Colloid Interface Sci Commun*. 2021 Nov 1;45:100519.
62. Martucci A, Braschi I, Bisio C, Sarti E, Rodeghero E, Bagatin R, et al. Influence of water on the retention of methyl tertiary-butyl ether by high silica ZSM-5 and Y zeolites: A multidisciplinary study on the adsorption from liquid and gas phase. *RSC Adv*. 2015;5(106):86997–7006.
63. Ross T. Indices for performance evaluation of predictive models in food microbiology. *J Appl Bacteriol*. 1996;81(5):501–8.
64. Motulsky HJ, Ransnas LA. Fitting curves to data using nonlinear regression: a practical and nonmathematical review. *FASEB J*. 1987;1(5):365–74.
65. Mishra SK. The Most Representative Composite Rank Ordering of Multi-Attribute Objects by the Particle Swarm Optimization [Internet]. Rochester, NY: Social Science Research Network; 2009 [cited 2025 Feb 20]. Available from: <https://papers.ssrn.com/abstract=1326386>
66. Kumar PS, Vasanthakumar sathya selva bala, Kirupha S, P. V, Sivanesan S. Adsorption equilibrium studies on copper (II) ions removal by natural waste using nonlinear approach. *Environ Eng Manag J*. 2011 Feb 1;10:285–95.
67. Dlugosz O, Szostak K, Matysik J, Matyjasik W, Banach M. Fabrication of ZnO/Ag and ZnO/Fe nanoparticles with immobilised peroxidase as a biocatalyst for photodegradation of ibuprofen. *Sustain Mater Technol*. 2023 Dec 1;38:e00763.
68. Melo JM, Lütke SF, Igansi AV, Franco DSP, Vicenti JRM, Dotto GL, et al. Mass transfer and equilibrium modelings of phenol adsorption on activated carbon from olive stone. *Colloids Surf Physicochem Eng Asp*. 2024 Jan 5;680:132628.
69. Sivarajasekar N, Baskar R. Adsorption of basic red 9 onto activated carbon derived from immature cotton seeds: isotherm studies and error analysis. *Desalination Water Treat*. 2014 Dec 6;52(40–42):7743–65.
70. Veličković ZS, Marinković AD, Bajić ZJ, Marković JM, Perić-Grujić AA, Uskoković PS, et al. Oxidized and ethylenediamine-functionalized multi-walled carbon nanotubes for the separation of low concentration arsenate from water. *Sep Sci Technol*. 2013 Sep 2;48(13):2047–58.
71. Mondal S, Sinha K, Aikat K, Halder G. Adsorption thermodynamics and kinetics of ranitidine hydrochloride onto superheated steam activated carbon derived from mung bean husk. *J Environ Chem Eng*. 2015 Mar 1;3(1):187–95.
72. Anirudhan TS, Deepa JR, Christa J. Nanocellulose/nanobentonite composite anchored with multi-carboxyl functional groups as an adsorbent for the effective removal of Cobalt(II) from nuclear industry wastewater samples. *J Colloid Interface Sci*. 2016 Apr 1;467:307–20.
73. da Rosa ALD, Carissimi E, Dotto GL, Sander H, Feris LA. Biosorption of rhodamine B dye from dyeing stones effluents using the green microalgae *Chlorella pyrenoidosa*. *J Clean Prod*. 2018 Oct 10;198:1302–10.
74. Torres-Caban R, Vega-Olivencia CA, Alamo-Nole L, Morales-Irizarry D, Roman-Velazquez F, Mina-Camilde N. Removal of copper from water by adsorption with calcium-alginate/spent-coffee-grounds composite beads. *Materials*. 2019 Jan;12(3):395.
75. Zhang M, Zhu L, He C, Xu X, Duan Z, Liu S, et al. Adsorption performance and mechanisms of Pb(II), Cd(II), and Mn(II) removal by a β -cyclodextrin derivative. *Environ Sci Pollut Res*. 2019 Feb 1;26(5):5094–110.
76. Chu KH, Debord J, Harel M, Bollinger JC. Mirror, Mirror on the Wall, Which Is the Fairest of Them All? Comparing the Hill, Sips, Koble–Corrigan, and Liu Adsorption Isotherms. *Ind Eng Chem Res*. 2022 May 18;61(19):6781–90.
77. Micheletti DH, Andrade JGS, Porto CE, Barros BCB, Rosa SLF, Sakai OA, et al. Valorization of agro-industrial wastes of sugarcane bagasse and rice husk for biosorption of Yellow Tartrazine dye. *Acad Bras Ciênc*. 2024 Dec 9;96:e20231308.
78. Sipos P. Searching for optimum adsorption curve for metal sorption on soils: comparison of various isotherm models fitted by different error functions. *SN Appl Sci*. 2021 Feb 27;3(3):387.
79. Zuo S, Sun Y, Zheng Y, Sun X, Hu J. Efficient selective uptake of Hg(II) using a porous organic polymer rich in N and S atoms. *J Environ Chem Eng*. 2024 Feb 1;12(1):111924.
80. Unuabonah EI, Adewuyi A, Kolawole MO, Omorogie MO, Olatunde OC, Fayemi SO, et al. Disinfection of water with new chitosan-modified hybrid clay composite adsorbent. *Heliyon* [Internet]. 2017 Aug 1 [cited 2025 Feb 17];3(8). Available from: [https://www.cell.com/heliyon/abstract/S2405-8440\(17\)30813-7](https://www.cell.com/heliyon/abstract/S2405-8440(17)30813-7)
81. Gupta A, Gupta N, Garg R, Kumar R. Evaluation, Selection and Ranking of Software Reliability Growth Models using Multi criteria Decision making Approach. In: 2018 4th International Conference on Computing Communication and Automation (ICCCA) [Internet]. 2018 [cited 2025 Feb 18]. p. 1–8. Available from: <https://ieeexplore.ieee.org/abstract/document/8777644>
82. Lambert RJW, Mytilinaios I, Maitland L, Brown AM. Monte Carlo simulation of parameter confidence intervals for nonlinear regression analysis of biological data using Microsoft Excel. *Comput Methods Programs Biomed*. 2012 Aug 1;107(2):155–63.